

Finite volume effects with stationary wave solution from Nambu–Jona-Lasinio model

Qing-Wu Wang^{1,*}, Yonghui Xia², Chao Shi², and Hong-Shi Zong^{2†}

¹*Department of Physics,
Sichuan University, Chengdu 610064, China*

²*Department of Physics,
Nanjing University, Nanjing 210093, China*

In this paper, we use the two-flavor Nambu–Jona-Lasinio (NJL) model with the proper time regularization to study the finite-volume effects of QCD chiral phase transition. Within a cubic volume of finite size L , we choose the stationary wave condition (SWC) as the real physical spatial boundary conditions of quark fields and compare our results with that by means of commonly used (anti-)period boundary condition (APBC or PBC). It is found that the results by means of SWC are obviously different to the results from the APBC or PBC. Although the three boundary conditions give the same chiral crossover transition curve in the infinite volume limit, the limit size L_0 (when $L \geq L_0$, the chiral quark condensate $-\langle\bar{\psi}\psi\rangle_L$ is indistinguishable from that at $L = \infty$) using SWC is $L_0 \approx 500$ fm which is much larger than the results obtained using APBC or PBC. More importantly, $L_0 \approx 500$ fm is also much large than the typical size of the quark-gluon plasma produced by the relativistic heavy ion collisions. This means that the finite volume effects play a very important role in Relativistic Heavy Ion Collisions. In addition, we also found that when $L \leq 2$ fm, even at zero temperature the chiral symmetry is effectively restored. Furthermore, to quantitatively reflect the finite volume effects on the QCD chiral phase transition, we introduce a new vacuum susceptibility, $\chi_{1/L}(T) = -\frac{\partial\langle\bar{\psi}\psi\rangle}{\partial(1/L)}$. With this new vacuum susceptibility, it is very interesting to find $\chi_{1/L}(T=0) = \chi_{1/L}(T=1/L)$ for SWC.

PACS numbers: 12.38.Mh, 11.10.Wx, 64.60.an

Dynamical chiral symmetry breaking (DCSB) is one of the key feature of Quantum Chromodynamics (QCD). The chiral phase transition at finite temperature is of continuous interests for studying the QCD phase diagram [1–4]. Many different methods have been used to analyse chiral symmetry breaking and restoration in variant situation. Other than color confinement, DCSB involving light degrees of freedoms which may propagate over long distances is thus closely relevant to the size of the system. In the early universe, a few microseconds after big bang, when the temperature was extremely high, the quark-gluon plasma (QGP) may have been prevalent. Experimentally, such a state can be reproduced in laboratory by relativistic heavy ion collisions (RHICs) [5, 6]. The matter formed due to the energy deposition of the colliding heavy ion obviously has a finite volume. Volume of homogeneity ranges between approximately $50 \sim 250$ fm³ for Au-Au and Pb-Pb collisions space, while volume of the smallest QGP system produced is estimated to be as low as $(2 \text{ fm})^3$ [7–9]. In view of the finite QGP size produced in RHICs can be compared with the wavelength of π meson, so it is very important to study phenomena related to the finite volume size. Actually, finite volume effects in QCD have already been studied for several decades [10]. The steady improvements of lattice simulations also make the calculations on finite volume effects possible and to give accurate results a thorough understanding of finite volume effects is needed.

Many different methods have been proposed to study the finite volume effects [11–19], and a recent summary is given in Ref.[10]. Within a finite volume, a concrete boundary condition needs to be chosen in advance. In the past, there are two typical boundary conditions: periodic boundary condition (PBC) and anti-periodic boundary condition (APBC), namely APBC for the quark fields and PBC for gluon fields. At finite temperature, it is claimed that the particle field should take the same boundary condition (PBC or APBC) in the spatial and temporal directions to ensure permutation symmetry. The quark-meson model gives results consistent with chiral perturbation theory with APBC [10]. Quark-meson model and lattice QCD simulation show results of low-energy behaviors depend on the choice of the quark boundary condition [15, 20–22], even though the lattice simulation still takes the PBC as a *de facto* standard [10, 22].

Before we discuss the finite-volume effects on QCD chiral phase transition, a brief retrospect of the finite volume effects on the black-body radiation is beneficial. As we all know, when the size of the black body cavity is large enough, the black-body radiation spectrum does not depend on the choice of the spatial boundary condition. That is, whether it is PBC, APBC or a stationary wave condition (SWC), none of the final results will be affected. But when the size of the black-body cavity is small enough, to ensure that photon gas is confined to

the cavity, people must use the SWC to study the finite volume effect on black body radiation. Therefore, in this article we will adopt the SWC to explore the finite volume effect on the QCD phase transition and compare our results with those by means of PBC and APBC used in the past.

We will calculate the finite-volume effects of QCD chiral phase transition with the three types of boundary in the framework of NJL model. The NJL model is a faithful phenomenological model of QCD [23, 24]. It provides insight into the quark flavor dynamics. The Lagrangian is

$$\mathcal{L}_{NJL} = \bar{\psi}(i\gamma_\mu)\partial^\mu - \hat{m}_q\psi + G[(\bar{\psi}\psi)^2 + (\bar{\psi}i\gamma_5\tau\psi)^2], \quad (1)$$

where G is the four-quark effective coupling. We consider only the u-d quark degree of freedom and work in the limit of exact isospin symmetry.

In the mean field approximation, the effective quark mass is $M = m + \sigma$ with

$$\sigma = -2G\langle\bar{\psi}\psi\rangle \quad (2)$$

and the chiral quark condensate is defined as

$$\langle\bar{\psi}\psi\rangle = -\int \frac{d^4p}{(2\pi)^4} \text{Tr}[S(p)], \quad (3)$$

where $S(p)$ is the dressed quark propagator and the trace is taken in color, flavor and Dirac spinor spaces.

Since the NJL model is non-renormalizable, a cut off on the momentum integration is usually implemented for regularization. There are many different regularization schemes and we will use the proper time regularization [4, 14, 15, 25–29] here. Under this regularization scheme the trace term in Eq.(3) is replaced by an integral with a suitable choice of the cutoff function. Here in the gap equation the key equation is a replacement $\frac{1}{A(p^2)^n} \rightarrow \frac{1}{(n-1)!} \int_{\tau_{UV}}^\infty d\tau \tau^{n-1} e^{-\tau A(p^2)}$. Then the chiral quark condensate in the infinite volume and at zero temperature can be written as

$$\begin{aligned} \langle\bar{\psi}\psi\rangle &= -N_c N_f \int \frac{d^4p}{(2\pi)^4} \frac{4M}{p^2 + M^2} \\ &= -24M \int_{-\infty}^\infty \frac{d^4p}{(2\pi)^4} \int_{\tau_{UV}}^\infty d\tau e^{-\tau(p^2 + M^2)} \\ &= -\frac{3M}{2\pi^2} \int_{\tau_{UV}}^\infty d\tau \frac{e^{-\tau M^2}}{\tau^2}. \end{aligned} \quad (4)$$

At finite temperature, the quark four-momentum is replaced by $p_k = (\vec{p}, \omega_k)$, with $\omega_k = (2k+1)\pi T$, $k \in \mathbb{Z}$ for fermion. The fourth momentum is replaced by a sum of all the fermion Matsubara frequencies ω_k . Then the two

quark condensate satisfies

$$\begin{aligned} \langle\bar{\psi}\psi\rangle &= -24M \int_{\tau_{UV}}^\infty d\tau e^{-\tau M^2} \times \\ &\quad T \sum_{k=-\infty}^\infty \int_0^\infty \frac{dp}{2\pi^2} p^2 e^{-\tau(p^2 + \omega_k^2)} \\ &= -\frac{3MT}{\pi^{3/2}} \int_{\tau_{UV}}^\infty d\tau \frac{e^{-\tau M^2}}{\tau^{3/2}} \theta_2(0, e^{-4\pi^2\tau T^2}), \end{aligned} \quad (5)$$

where the Jacobi function is defined as $\theta_2(0, q) = 2\sqrt{q} \sum_{n=0}^\infty q^{n(n+1)}$. Then the constituent quark mass is

$$M = m + \frac{6GMT}{\pi^{3/2}} \int_{\tau_{UV}}^\infty d\tau \frac{e^{-\tau M^2}}{\tau^{3/2}} \theta_2(0, e^{-4\pi^2\tau T^2}). \quad (6)$$

At finite volume, the quark momentum is discretized and the integral over all spatial momenta is replaced by a sum over discrete momentum modes. The discrete momenta depending on the boundary conditions are

$$\vec{p}_{PBC} = \frac{4\pi^2}{L^2} \sum_{i=1}^3 n_i^2, \quad n_i = 0, \pm 1, \pm 2 \dots \quad (7)$$

$$\vec{p}_{APBC} = \frac{4\pi^2}{L^2} \sum_{i=1}^3 (n_i + \frac{1}{2})^2, \quad n_i = \pm 1, \pm 2 \dots \quad (8)$$

$$\vec{p}_{SWC} = \frac{\pi^2}{L^2} \sum_{i=1}^3 n_i^2, \quad n_i = +1, +2, +3 \dots \quad (9)$$

where L is the cubic volume size. The integration measure is replaced by sum of discrete momenta

$$\int dp(\dots) \rightarrow \frac{2\pi}{L} \sum_{n_i}(\dots). \quad (10)$$

Then the constituent quark mass is constrained by

$$\begin{aligned} M &= m + 48GM \int_{\tau_{UV}}^\infty d\tau e^{-\tau M^2} [T \times \\ &\quad \sum_{k=-\infty}^\infty e^{-\tau\omega_k^2} \prod_{i=1}^3 \sum_{n_i} e^{-\tau p_i^2}] \\ &= m + 48GMT \int_{\tau_{UV}}^\infty d\tau e^{-\tau M^2} \times \\ &\quad \theta_2(0, e^{-4\pi^2\tau T^2}) \left[\frac{f(\theta)}{L}\right]^3, \end{aligned} \quad (11)$$

with

$$f(\theta) = \begin{cases} \theta_2(0, e^{-4\tau\pi^2/L^2}) & \text{for APBC;} \\ \theta_3(0, e^{-4\tau\pi^2/L^2}) & \text{for PBC;} \\ \theta_3(0, e^{-4\tau\pi^2/L^2}) - 1 & \text{for PBC-0;} \\ [\theta_3(0, e^{-4\tau\pi^2/L^2}) - 1]/2 & \text{for SWC.} \end{cases} \quad (12)$$

Here we use PBC-0 to represent PBC without the zero-mode contribution (PBC would require an additional explicit treatment of the fermionic zero mode) and the $\theta_3(0, q) = 1 + 2 \sum_{n=1}^\infty q^{n^2}$.

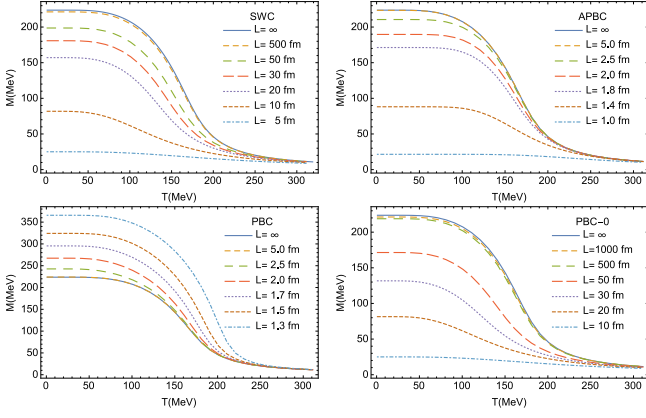


FIG. 1: Quark mass as a function of temperature and L . In contrast to SWC and APBC, the quark mass obtained from PBC increases as the volume decreases, owing to the zero-momentum contribution.

The parameters we used here are $m = 5$ MeV, $G = 3.26 \times 10^{-6}$ MeV $^{-2}$, $\Lambda_{UV} = 1080$ MeV and the τ_{UV} is given by $1/\Lambda_{UV}^2$. With these parameters the quark mass is $M = 223.7$ MeV at zero temperature. In all the calculations we neglect the possible dependence of the coupling on temperature and condensate which is discussed in Refs. [30–32]. Also the effective coupling constants does not depend on the volume size [33] in this work.

The quark mass M at different L and temperature under different boundary conditions are plotted in Fig.(1), with a few things noticeable. Firstly, for SWC, APBC and PBC-0, the figures show crossover of chiral phase transitions. When the volume size L is not very small, the quark mass or the chiral quark condensate smoothly reduces as the temperature increases. The three boundary conditions give same results in the thermodynamic limit. In addition, for APBC, when $L \geq L_0 = 5$ fm (L_0 is called the limit size)), the quark mass is indistinguishable from that at $L = \infty$ which is consistent with result from Ref.[18]. While for SWC, it is found that the corresponding $L_0 = 500$ fm. Both APBC and SWC the quark mass decreases as volume size decreases. These results are qualitatively consistent with those from Dyson-Schwinger equation with APBC [18, 19]. Secondly, for PBC, when the volume size L decreases, the quark mass increases which is totally different with results from the other two boundary conditions. This is an effect of fermionic zero mode that is present for PBC. Thirdly, when the volume size $L \leq 2$ fm, there is only Wigner-Weyl solution for the case of SWC, where the dynamic chiral symmetry is total restored. But, for PBC, The dynamical chiral symmetry breaking always exists for arbitrary L at zero temperature. It is obvious that the choice of boundary conditions has a significant effect on the finite-volume mass shift.

The zero momentum contribution to the quark mass with PBC can be observed through the gap equation Eqs.(11) and (12). The term $f(\theta)/L$ diverges as $L \rightarrow 0$

only for PBC with a zero mode. Without mechanism to restore the chiral symmetry, quark mass M is nonzero and chiral condensate from the gap equation has a solution of negative infinity at low temperature. At very high temperature, the zero momentum contribution is heavily suppressed by the term $\theta_2(0, e^{-4\pi^2\tau T^2})$ and then the dynamical chiral symmetry gets restored.

The reason of these differences for different choice of boundary condition can be illustrated by Fig.(2). It is a plot of function $[f(\theta)/L]^{3/2}$ with $k = \tau\pi^2 = 20$. We have found that for any value of k , the relative positions of those curves keep invariant. For a fixed L , the order of curves along the vertical axis of Fig.(2) is also the order for quark mass in different boundary condition. From Eq.(11), as M is much large than current quark mass m and temperature is fixed, we reach to a relation

$$e^{\sqrt{\tau}M} \sim \left[\frac{f(\theta)}{L} \right]^{\frac{3}{2}}. \quad (13)$$

In Fig.(2), only the curve of PBC is a monotonically decreasing function of L . This explains why the effective quark mass increases as L decreases for PBC. The curves of PBC and APBC always reach the same limit as L increases and to approach their thermodynamic limit. The L_0 for PBC or APBC is much smaller than the one for SWC and PBC-0, which can explains the different behaviors of quark mass with different boundary conditions. The large value of function $[f(\theta)/L]^{3/2}$ means more quark field momenta are “squeezed” in unit volume which leads to an increase of chiral condensate and then constituent quark mass.

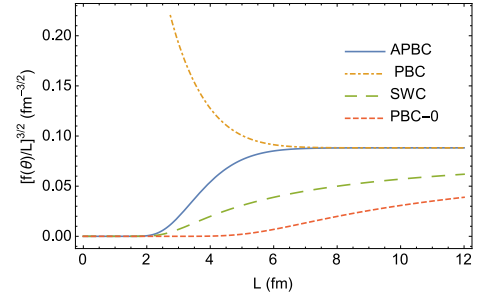


FIG. 2: The momentum summation as a function of volume size L for different boundary conditions.

The crossover behavior of quark chiral condensate can be depicted by the chiral quark condensation with respect to temperature and current quark mass. The chiral quark condensation with respect to temperature is defined as

$$\chi_T(T) = -\frac{\partial \sigma}{\partial T}. \quad (14)$$

The susceptibility with respect to current quark mass can be easily derived from Eq.(11) as all the parameters are fixed. But direct derivation of Eq.(11) give $\chi_m(T)$

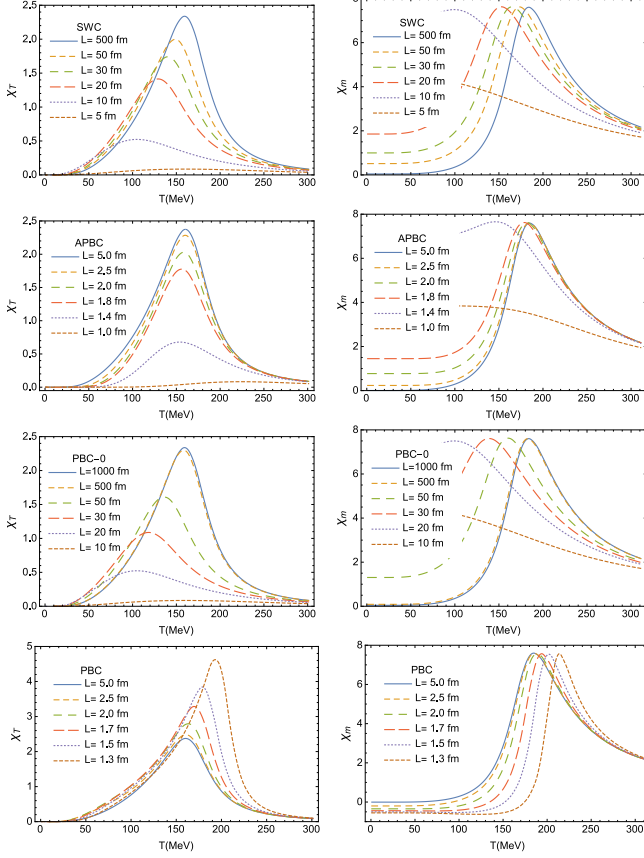


FIG. 3: Chiral susceptibilities as function of temperature at different volumes. χ_T and χ_m are the susceptibilities with respect to temperature and current quark mass respectively.

nonzero in the infinite volume at zero temperature. Actually, in the proper time regularization, parameters m , G and Λ_{UV} are fixed by experimental values of decay constant and mass of pion. Therefore if the coupling G is fixed, the ultraviolet cutoff Λ_{UV} must have dependence on the current quark mass m . In this consideration, we give a small change δ_m to m and get new cutoff $\Lambda_{UV}(m + \delta_m)$. Then the $\chi_m(T)$ can be deduced from formula

$$\chi_m(T) = \frac{\sigma(m + \delta_m) - \sigma(m)}{\delta_m}. \quad (15)$$

The results for the susceptibilities are showed in Fig.(3). The two kinds of susceptibility have different behaviors when the volume size L becomes very small. At zero temperature, the susceptibility χ_T is zero in any boundary condition and unaffected by the size of the boundary, but the susceptibility χ_m increases (decreases) as L decreases for APBC (PBC). Note that χ_m changes the sign as L decreases for PBC.

In the infinite volume limit and chiral limit, the sharp peak in the chiral susceptibility plot define the phase transition point. While beyond the chiral limit, we still take the chiral susceptibility as the order parameter and

TABLE I: Pseudo-critical temperature deduced from the susceptibilities $\chi_m(T)$ and $\chi_T(T)$. The temperatures are in unit MeV and volume size L is in unit fm.

SWC	L	500	50	30	20
	T_c^m	184	173	165	153
	T_c^T	164	153	145	134
PBC-0	L	500	50	30	20
	T_c^m	183	160	139	93
	T_c^T	163	142	118	94
APBC	L	5.0	2.5	2.0	1.8
	T_c^m	185	184	182	179
	T_c^T	165	165	163	161
PBC	L	5.0	2.5	2.0	1.7
	T_c^m	185	186	188	194
	T_c^T	165	166	168	175

use the maximum to find the pseudo-transition temperature. The pseudo-critical temperatures defined from the susceptibilities are denoted as T_c^m and T_c^T . In the infinite volume limit, $T_c^m \simeq 165\text{MeV}$ and $T_c^T \simeq 185\text{ MeV}$. This difference also exists in finite volume. Tab. I shows the pseudo-critical temperature at different volumes. For a specific boundary condition, the pseudo-critical temperatures χ_m and χ_T respond to the volume size in the same way. For SWC, the T_c^m and T_c^T decrease with smaller L while for PBC the T_c^m and T_c^T increase as L decreases. For APBC, T_c^m and T_c^T only slightly decreases with the decrease of L which is consistent with the result in Ref. [15] with large current quark mass.

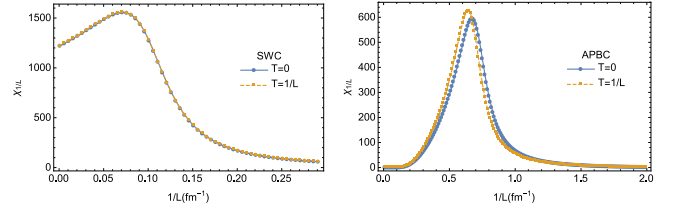


FIG. 4: The vacuum susceptibility with respect to volume size $1/L$. For quark field for SWC, the $T = 0$ and $T = 1/L$ curves coincide and the dynamical chiral symmetry is restored at $L = 2\text{ fm}$.

In order to quantitatively reflect the finite volume effects on the QCD chiral phase transition, similar to the chiral quark condensation with respect to temperature, here we introduce a new vacuum susceptibility, which is defined as the derivative of the chiral quark condensation with respect to spatial size $1/L$. We call it spatial susceptibility which reads as

$$\chi_{1/L}(T) = -\frac{\partial \sigma}{\partial (1/L)}. \quad (16)$$

According to the illustration, see Fig. (4), it is em-

phasized that in the Euclidean space, the discretization in the temporal direction (temperature T) and the discretization in the spatial direction ($1/L$) are equivalent. That is, as the temperature T or $1/L$ increases, chiral symmetry will be partially restored.

In summary, we have used the NJL model to study the chiral crossover transition in a finite volume. Besides the two commonly used APBC and PBC, we have chosen the SWC for the quark field as a real physical boundary condition. It is found that different boundary choice for the finite volume has dramatically influence on the QCD chiral behavior. Starting from the infinite volume, only PBC gives quark mass that increases as the volume size decreases and the chiral susceptibility $\chi_m(T)$ become negative at low temperature. The strange behavior of chiral quark condensate for PBC is due to dominant contribution from the zero mode at small L . In order to avoid this strange behavior, we use PBC-0 to represent the period boundary condition without the zero-mode contribution. Finally, we found that the results from PBC-0 are similar to that from SWC.

Here it should be noted that the results by means of SWC are obviously different to the results from the APBC and PBC. Although the three boundary conditions give the same chiral crossover transition curve in the infinite volume limit, the limit size L_0 using SWC is $L_0 \approx 500$ fm which is much larger than the results obtained using PBC or APBC. Especially important, $L_0 \approx 500$ fm is also far greater than the current maximum size in lattice simulations of full QCD in numerical calculations.

In the past it is hard to conceive of systems that are small enough to lead to observable finite-volume effects, since the length scales involved are so small compared to the typical extent of the system. However the experiment with relativistic heavy ion collisions has changed a lot. At present the estimated volume of QGP in RHICs is ~ 250 fm³ which can be compared with the wave length of the π meson. This means that the finite volume effects should be observed experimentally in RHICs. According to our calculation, the finite-volume effects may play a significant role in the QGP. Furthermore, a new spatial susceptibility reflecting the finite-volume effects of the chiral restoration in QGP was introduced and it was found that the finite-volume effects and the temperature effects were completely equivalent, namely for very small volume size or large temperature, chiral symmetry is effectively restored.

This work is supported in part by the National Natural Science Foundation of China (under Grants No.11475085, No.11535005 and 11690030).

[†] Email: zonghs@nju.edu.cn

- [1] A. M. Halasz, A. D. Jackson, R. E. Shrock, M. A. Stephanov, and J. J. M. Verbaarschot, Phys. Rev. **D58**, 096007 (1998).
- [2] Y. Aoki, G. Endrodi, Z. Fodor, S. D. Katz, and K. K. Szabo, Nature **443**, 675 (2006).
- [3] G. S. Bali, F. Bruckmann, G. Endrodi, Z. Fodor, S. D. Katz, and A. Schafer, Phys. Rev. **D86**, 071502 (2012).
- [4] Z. F. Cui, J. L. Zhang, and H. S. Zong, Sci. Rep. **7**, 45937 (2017).
- [5] J. Adams et al. (STAR), Nucl. Phys. **A757**, 102 (2005).
- [6] E. Shuryak, Prog. Part. Nucl. Phys. **62**, 48 (2009).
- [7] S. A. Bass et al., Prog. Part. Nucl. Phys. **42**, 313 (1999).
- [8] L. F. Palhares, E. S. Fraga, and T. Kodama, J. Phys. **G38**, 085101 (2011).
- [9] G. Graef, M. Bleicher, and Q. Li, Phys. Rev. **C85**, 044901 (2012).
- [10] B. Klein, Phys. Rept. **707**, 1 (2017).
- [11] M. E. Fisher and M. N. Barber, Phys. Rev. Lett. **28**, 1516 (1972).
- [12] J. Gasser and H. Leutwyler, Phys. Lett. **B184**, 83 (1987).
- [13] J. Gasser and H. Leutwyler, Nucl. Phys. **B307**, 763 (1988).
- [14] J. Braun, B. Klein, and H. J. Pirner, Phys. Rev. **D71**, 014032 (2005); **D72**, 034017 (2005).
- [15] J. Braun, B. Klein, H. J. Pirner, and A. H. Rezaeian, Phys. Rev. **D73**, 074010 (2006).
- [16] G. Colangelo, S. Durr, and C. Haefeli, Nucl. Phys. **B721**, 136 (2005).
- [17] G. Colangelo, A. Fuhrer, and S. Lanz, Phys. Rev. **D82**, 034506 (2010).
- [18] J. Luecker, C. S. Fischer, and R. Williams, Phys. Rev. **D81**, 094005 (2010).
- [19] B. L. Li, Z. F. Cui, B. W. Zhou, A. Sun, L. P. Zhang, and H. S. Zong, (2017), arXiv:1711.04914 [hep-ph].
- [20] D. B. Carpenter and C. F. Baillie, Nucl. Phys. **B260**, 103 (1985).
- [21] M. Fukugita, M. Okawa, and A. Ukawa, Nucl. Phys. **B337**, 181 (1990).
- [22] S. Aoki, T. Umemura, M. Fukugita, N. Ishizuka, H. Mino, M. Okawa, and A. Ukawa, Phys. Rev. **D50**, 486 (1994).
- [23] S. P. Klevansky, Rev. Mod. Phys. **64**, 649 (1992).
- [24] M. Buballa, Phys. Rept. **407**, 205 (2005).
- [25] S. B. Liao, Phys. Rev. **D53**, 2020 (1996).
- [26] D. F. Litim and J. M. Pawłowski, Phys. Lett. **B516**, 197 (2001).
- [27] D. Zappala, Phys. Rev. **D66**, 105020 (2002).
- [28] Z. F. Cui, Y. L. Du, and H. S. Zong, Int. J. Mod. Phys. Conf. Ser. **29**, 1460232 (2014).
- [29] J. L. Zhang, Y. M. Shi, S. S. Xu, and H. S. Zong, Mod. Phys. Lett. **A31**, 1650086 (2016).
- [30] Z. F. Cui, C. Shi, W. M. Sun, Y.-L. Wang, and H.-s. Zong, Eur. Phys. J. **C74**, 2782 (2014).
- [31] Q. W. Wang, Z. F. Cui, and H. S. Zong, Phys. Rev. **D94**, 096003 (2016).
- [32] A. Ayala, C. A. Dominguez, L. A. Hernandez, M. Loewe, A. Raya, J. C. Rojas, and C. Villavicencio, Phys. Rev. **D94**, 054019 (2016).
- [33] J. Gasser and H. Leutwyler, Phys. Lett. **B188**, 477 (1987).

* Email: qw.wang@scu.edu.cn